

Comparison of the Isothermal Oxidation Behavior of As-Cast Cu-17%Cr and Cu-17%Cr-5%Al Part II: Scale Microstructures

S. V. Raj[#]

NASA Glenn Research Center, MS 106-5, 21000 Brookpark Road, Cleveland, OH 44135

ABSTRACT

The isothermal oxidation kinetics of as-cast Cu-17%Cr and Cu-17%Cr-5%Al in air were studied between 773 and 1173 K under atmospheric pressure. Details of the oxidation kinetics of these alloys were discussed in Part I. This paper analyzes the microstructures of the scale and its composition in an attempt to elucidate the oxidation mechanisms in these alloys. The scales formed on Cu-17%Cr specimens oxidized between 773 and 973 K consisted of external CuO and subsurface Cu₂O layers. The total thickness of these scales varied from about 10 μm at 773 K to about 450 μm at 973 K. In contrast, thin scales formed on Cu-17%Cr-5%Al alloys oxidized between 773 and 1173 K. The exact nature of these scales could not be determined by x-ray diffraction but energy dispersive spectroscopy analyses were used to construct a scale composition map. Phenomenological oxidation mechanisms are proposed for the two alloys.

Keywords

Isothermal oxidation; Cu-Cr alloys; Cu-Cr-Al; copper alloys; oxidation kinetics;

Tel.: (216) 433-8195; Fax: (216) 433-5544; e-mail: sai.v.raj@nasa.gov

1. Introduction

In part I, the oxidation kinetics of Cu-17%Cr¹ and Cu-17%Cr-5%Al were compared and discussed. It was demonstrated that the addition of 5%Al to the Cu-17%Cr significantly improved its oxidation properties. In contrast to Cu-17%Cr, which exhibited parabolic oxidation behavior similar to pure Cu [1,2,3,4,5,6,7,8,9,10,11], Cu-Al [11,12,13], and several Cu-Cr [7,9] alloys, the oxidation behavior of Cu-17%Cr-5%Al is better represented by either a combination of parabolic and quartic equations or a logarithmic equation. The ternary phase diagrams [14,15], as well as the microstructural observations shown in Fig. 1 of part I, confirm that the alloy consists of a two-phase microstructure consisting of phases rich in Cr and Cu.

Microstructural observations on Cu-Al alloys containing between 1 and 4%Al oxidized in air up to 1273 K revealed that alloys containing less than 2%Al form a thick external porous oxide scale consisting mainly of Cu₂O with traces of CuO and CuAlO₂ dispersed within it above 1073 K with considerable internal oxidation of the matrix [13]. A continuous protective alumina scale was observed only for the Cu-4%Al alloy above 973 K oxidized in pure oxygen. Recent limited studies on the oxidation behavior of Cu-2 to 4(at.%)Al and Cu-4 to 8(at.%)Cr-2 to 4%Al alloys at 1073 K indicate that these alloys form an outer CuO external scale and an inner Al₂O₃ scale at the interface with the unoxidized matrix after 24 h [11,12]; a transition subsurface layer consisting of CuO and (Cr,Al)₂O₃ formed between the external and innermost scales. It was observed that the continuity of the subsurface alumina scale depended on the amount of Cr present in the alloy although it was observed in all the Cr containing alloys. However, this study was limited to a single temperature of 1073 K [11,12].

¹ All compositions reported in the paper are in wt.% unless otherwise noted.

The objectives of the present paper are to understand the effect of 5% Al on the scale compositions microstructures formed on Cu-17%Cr and Cu-17%Cr-5%Al to compliment the oxidation data reported for these two alloys in part I. No similar comparisons appear to have been reported for these alloys.

2. Experimental Procedures

Details of the alloy preparation procedures, compositions of the alloys and the oxidation tests were reported in part I. The oxidation tests were conducted between 773 and 1173 K for 100 h under dry flowing oxygen at 0.1 MPa, where the flow rate of the gas was 100 standard ccm. In the case of the Cu-17%Cr specimens, tests were conducted at absolute temperatures, T, between 773 and 973 K since there were insufficient good specimens to conduct tests at 1073 and 1173 K. The nature of the oxide scales were characterized by x-ray diffraction (XRD) after oxidation for 100 h. The specimens were vacuum infiltrated in an epoxy mount to protect the scales and then carefully cut in half by a diamond saw. One of the halves retained in its epoxy mount was re-mounted by vacuum infiltration in a new epoxy mount for viewing its oxidized cross-section. Microstructural observations were conducted by optical and field emission scanning electron microscopy (FESEM), back scattered electron (BSE) imaging and energy dispersive spectroscopy (EDS).

3. Results

3.1 X-ray diffraction analyses

Table 1 shows the XRD results of the surface oxide scales formed on the Cu-17%Cr and Cu-17%Cr-5%Al specimens after 100 h at temperature. The scale formed at the surface of the

Cu-17%Cr specimen oxidized at 773 K consisted of a mixture of Cu₂O and CuO with small amounts of α -Cr and α -Cu. However, the oxidation of Cu-17%Cr at 873 and 973 K resulted in a scale composition consisting primarily of CuO with Cu₂O being detected only as a minor constituent. In contrast, the scales formed on the Cu-17%Cr-5%Al consisted of a mixture of α -Cr and α -Cu with a weak CuO peak being detected for the specimen oxidized at 1073 K. Based on the XRD results discussed by Chiang *et al.* [16], as well as on the Cu-Cr-Al ternary phase diagrams [14,15], it is reasonable to conclude that this α -Cu phase is rich in Al. The presence of either Al₂O₃ or Cr₂O₃ was not detected in the surface oxide scales for both alloys.

3.2 Microstructural observations

3.2.1 Cu-17%Cr

Figures 1(a-c) show low magnification optical micrographs of the oxide scales formed on the surfaces of Cu-17%Cr oxidized between 773 and 973 K for 100 h. The alloy formed an extensive oxide scale between 773 and 973 K with large amounts of cracks and voids observed both in the scale and at the oxide layer-matrix interfaces. The unoxidized microstructures of the specimens consisted of α -Cu matrix and α -Cr second phase (see part I). A close examination of the oxidized edges revealed that the scales had grown outward away from the original free surface since the outer oxide layers were completely devoid of Cr-rich particles (Fig. 2). Significantly, the Cr-rich particles left in the matrix were surrounded by a large amount of voids presumably due to the migration of Cu to the free surface.

Back scattered electron image (Fig. 3(a)) and EDS analyses (Figs. 3(b-d)) of the scales revealed that the scale compositions were similar between 773 and 973 K consisting of a dark

gray outer layer rich in oxygen lying over a light gray subsurface layer exhibiting weaker oxygen spectral peak. Since both layers were Cu-rich and contained undetectable amounts of Cr, it is reasonable to assume that these dark and light gray oxides are CuO and Cu₂O, respectively. It is important to note that the energy levels for the Cr L_α and O K_α lines are close to each other so that the EDS spectra from these elements cannot be easily separated (Fig. 3(d)). Figure 3(e) shows the EDS data from an area of the matrix below the scale, where only Cu peaks are observed. Interestingly, long cracks approximately parallel to the free surface were often observed in the oxide scales these specimens presumably due to lineal and volumetric dimensional changes brought about by the kinetics of oxide nucleation and growth (Fig. 2).

A continuous protective layer of Cr₂O₃ was not observed in any of the specimens investigated in the present study despite the presence of large amount of α-Cr particles in them (Figs. 4(a-d)). Owing to the closeness of the Cr L_α and O K_α energy spectra, the bright regions corresponding to Cr-particles in the oxygen x-ray dot map probably represent Cr L_α rather than O K_α reflections (Fig. 4(c)). The observation of a large amount of voids near these α-Cr particles (Figs. 2 & 3(a)) and the fact that the EDS analyses of outer oxide layers consist solely of Cu with an absence of Cr peaks (Fig. 3(b)) can be attributed to the relatively rapid diffusion of Cu to the outer free surfaces at these temperatures. The morphology of the oxide scales changed from undulating layers with nonuniform thickness at 773 K (Fig. 5(a)) to layers with greater degrees of uniformity in their thicknesses (Figs. 5(b) & (c)). An examination of Fig. 5 reveals that the external CuO layer exhibits an increasing tendency towards columnar growth as the oxidation temperature increases from 773 to 973 K.

3.2.2 Cu-17%Cr-5%Al

Figures 6(a-d) show the SEM and BSE microstructures of the cross-sections of the specimens oxidized at 773 and 1173 K as examples of the scale morphologies at the two extreme temperatures. Once again, the matrix consists of α -Cu and α -Cr particles. In contrast to Cu-17%Cr, the oxide scale at the free surface of the Cu-17%Cr-5%Al alloy was extremely thin and not easily discernable in many areas of the specimen especially in the BSE mode. The scale thickness was non-uniform and discontinuous in the specimens oxidized at 773 K (Fig. 7(a)) and 873 K (Fig. 7(b)). The uniformity in the thickness of the scale and the degree of its continuity increased with increasing temperature. Importantly, unlike Cu-17%Cr, no voids were observed in the microstructures of the specimens tested between 773 and 1173 K.

Energy dispersive spectroscopy analyses of the scales and surface regions revealed a qualitative increase in the Al content of the oxide scale with increasing temperature. At 773 K, the scale thickness was too thin in most areas to obtain a reliable EDS analysis. However, an EDS analysis of the scale obtained in one region of the specimen (Fig. 8(a)) revealed that it was richer in Cu than Al (Fig. 8(b)); the spectra from the matrix are shown in Fig. 8(c). At 873 K, the composition of the outer scale corresponding to region E in Fig. 9(a) was generally rich in Cu and O (Fig. 9(b)) while an inner subsurface layer corresponding to region F was a mixed (Al, Cu) oxide (Fig. 9(c)). The spectra from region G in Fig. 9(a) lying more than 1 μm from the outer surface showed only Al and Cu peaks with an insignificantly small oxygen peak (Fig. 9(d)). It is worth noting that isolated islands of the outer scale had a significant amount of Al in them. Surprisingly, Cr peaks were not frequently observed in the scale. It is unclear whether the general absence of Cr peaks in the scale was influenced by the local composition of the

underlying matrix. At 973 K, both the inner and outer scale corresponding to regions D and B in Fig. 10(a) consist of (Al,Cu) oxides with the Al and Cu peaks being significantly higher and lower, respectively, in the inner than in the outer scale; the oxygen content in region C is very small (Fig. 10(b-d)). This subsurface enrichment of the scale in Al is clearly depicted in the elemental x-ray maps (Fig. 11(a-e))².

The scale composition was varied at 1073 K, where the scales consisted of either Al-rich or Cr-rich oxides with only small amounts of Cu present in both types of scales (Figs. 12(a-f))³. Figure 12(a) shows a BSE image of the scale with the matrix spectra from region A shown in Fig. 12(b). The energy dispersive spectra obtained from region B reveals that the oxide scale is richer in Cr than Al in the subsurface area adjacent to the matrix (Fig. 12(c)). In contrast, region C lying closer to the external surface is richer in Al than Cr (Fig. 12(d)). Regions D and E exhibit strong Al, Cr and O peaks thereby indicating that these are mixed oxides with the height of the Al peak being higher in region D than in region E and the Cr peak being higher in the latter region than in the former area (Figs. 12(e) & (f)). These observations suggest that the scale composition gradually transitions from chromia to alumina during the course of oxidation of the alloy at this temperature. This transition is complete within 100 h at 1173 K, where the scale composition is predominantly Al-rich containing only small amounts of Cr and Cu (Figs. 13(a) & (b)).

² The x-ray dot maps show that the particle at the bottom of Fig. 11(a) was deficient in Al, Cr, Cu and Si but rich in O. It is concluded that the particle is a contaminant from the alloy preparation process.

³ Although the Cr L_{α} and O K_{α} peaks overlap, the peak identifications shown in Figs. 12(c-f) denote only the strongest likely contributor. The source of Si in the spectra is probably due to residual colloidal silica left over from the metallographic preparation process.

4. Discussion

It was demonstrated in part I that the oxidation behavior of Cu-17%Cr is similar to that of pure Cu. The compositions of the scale formed at the surfaces of the alloy consisted of an external layer of CuO and a subsurface layer of Cu₂O consistent with those observed in pure Cu oxidized in air or oxygen at 0.1 MPa pressure [1,2,3,4,5,6,7,9,10,11]. The present observations, which are consistent with those on Cu-1%Al [11,13] and Cu-Cr [6] alloys, suggest that the presence of large α -Cr particles in the alloy had no significant effect on the oxidation behavior of the alloy. This observation is confirmed by the fact that a continuous protective Cr₂O₃ was not observed in any of the as-cast Cu-17%Cr specimens after oxidation between 773 and 973 K (Figs. 1-3). Instead, there was considerable evidence that the α -Cr particles had undergone internal oxidation (Fig. 4).

In contrast to the oxidation behavior of Cu-17%Cr, it was reported in part I that Cu-17%Cr-5%Al exhibited excellent oxidation resistance by several orders of magnitude compared to Cu-17%Cr. It was also shown that the addition of 5% Al resulted in a change in the oxidation kinetics either from parabolic to quartic or alternatively to logarithmic rate behavior consistent with those reported for Cu-Al alloys containing Al > 2.5% [13]. The effect of adding 5% Al to the base Cu-17%Cr alloy resulted in a thin scale, which was not easily discernable at low magnifications. In contrast, the thickness of the scales formed on Cu-17%Cr oxidized between 773 and 973 K varied between 10 and 400 μ m, respectively. Since the scales were thin and nonuniform below 973 K, the compositions of the oxides could not be determined by XRD (Table 1) or accurately analyzed by electron microprobe techniques. As a result, the scale

composition is hypothesized as described in Sec. 4.1 from the characteristics of several EDS spectra obtained from random locations for each specimen.

4.1 Scale composition map for Cu-17%Cr-5%Al

Figure 14 summarizes the EDS results in an oxide scale composition map represented as a plot of the absolute oxidation temperature against the local distance, x , with $x = 0$ demarcating the scale-matrix interface. Owing to the fact that the scales were not always discernable, it was felt that obtaining an average scale thickness would not be meaningful. Since the interfaces between the scale and the unoxidized matrix were not always planar especially at the higher temperatures, the scale thickness was locally measured along an arbitrary line drawn perpendicular to the interface in the field of view where the EDS analysis was conducted. The EDS analyses were conducted at each temperature in several different areas of the specimen and the thicknesses of the oxide layers were measured at these local points. Since the peak height for each element varied from one EDS spectrum to another, the convention followed in this paper identifies the oxides based on their relative heights. Thus, $(Al,Cr,Cu)_2O$ suggests the Al spectral peak was the highest and that for Cu was the smallest whereas $(Cu,Al)_2O$ denotes that the spectral peak for Cu was higher than that for Al. As noted earlier in Table 1, the XRD data of the oxidized specimens did not provide any insights on the stoichiometric compositions of the oxides. Thus, the regions of different scale compositions indicated in Fig. 14 are shown to be consistent with the present EDS results. These observations are also consistent the observed compositions of the oxide scales formed on Cu and Cu-17%Cr. For simplicity, this paper assumes that the oxides in the scales consist primarily of M_2O and M_2O_3 , where M is one or more combinations of Al, Cr and Cu, although it is possible other mixed oxides may have

formed [13]. In the absence of the inability to determine the precise stoichiometric compositions of the oxides forming the scale, this assumption is reasonable.

An examination of Fig. 14 reveals that the Al and Cr contents of the outer scale gradually increase while the amount of Cu correspondingly decreases with increasing test temperature; the subscale elemental compositions also undergo similar variations. The outer scale is essentially CuO at and below 973 K, which transitions to mixed oxides consisting of Al and Cu in the subsurface scale layers with the innermost layers close to the matrix being richer in Al. These results indicate that Cu diffusion from the matrix to the free surface is faster than Al at these temperatures. Significantly, no Cr is observed in the scale composition at these temperatures. This observation is due in part to the absence of α -Cr particles in area of analysis and in part due to low diffusivity of Cr at these temperatures. At higher temperatures, the Cu content in the scales decreases and becomes negligible above 1073 K as Al and Cr replace Cu due to their increased rate of diffusion from the matrix to the free surface. Thus, the $(\text{Al,Cr,Cu})_2\text{O}$ mixed oxide⁴ outer scale is replaced by protective $(\text{Cr,Al})_2\text{O}_3$ and Al_2O_3 subsurface scale layers above 973 K.

4.2 Phenomenological mechanisms

As reported in Sec. 3.2, the microstructures of the oxidized Cu-17%Cr and Cu-17%Cr-5%Al specimens differed from each other in two significant ways. First, Cu-17%Cr specimens formed thick copper oxide scales (Figs. 1-4), whereas the scales formed on Cu-17%Cr-5%Al specimens were thin mixed oxide scales containing various amounts of Al, Cr and Cu (Figs.

⁴ The $(\text{Al,Cr,Cu})_2\text{O}$ rather than $(\text{Al,Cr,Cu})\text{O}$ is used since earlier research on pure Cu suggests that Cu_2O is more likely to form than CuO with increasing temperature and decreasing pressure of oxygen [4,6].

6,8,9,11-14). Second, the Cr-rich precipitates in oxidized Cu-17%Cr specimens were typically surrounded by voids (Figs. 2 & 3). In contrast, no voids were observed around the Cr-rich particles in the oxidized Cu-17%Cr-5%Al specimens (Figs. 6 & 7(b)). The latter observation suggests that the addition of Al to Cu-17%Cr has the additional beneficial effect of suppressing void formation and growth in the matrix. The observation of voids in the Cu-17%Cr can be attributed to the formation of vacancies in the matrix as Cu atoms diffuse to the matrix/oxide interface during oxidation and their subsequent agglomeration at the α -Cr/matrix and other interfaces to nucleate voids. Clearly, the addition of Al appears to affect this vacancy agglomeration and subsequent void nucleation in the Cu-17%Cr-5%Al alloy during oxidation.

In order to understand the differences in the oxidation behavior of these two alloys, two phenomenological models are proposed in this section. The oxidation of pure Cu occurs by the diffusion of copper atoms through the Cu_2O , where this diffusion is facilitated by copper vacancies [17]. As virgin Cu-17%Cr oxidizes (Fig. 15(a)), Cu atoms migrate towards the free surface leaving behind vacancies on copper lattice sites, V_{Cu} (Fig. 15(b)). The Cu vacancies migrate to the free surface and to the α -Cr/ α -Cu interfaces in the specimen ultimately aggregating to form voids. The Cu atoms react with oxygen at the free surface forming first a layer of Cu_2O , which on further oxidation results in the formation of an external CuO scale (Fig. 15(c) & (d)). Columnar grains in the CuO layer grow transverse to the oxide/matrix interface presumably due to the relatively large temperature gradient between metal surface and the interior temperature. A continuous protective Cr_2O_3 layer does not form as a subsurface layer.

The oxidation of virgin Cu-17%Cr-5%Al (Fig. 16(a)) results in the formation of a thin scale at the temperatures investigated in this study. As demonstrated in part I, the initial stages of oxidation are well represented by a parabolic oxidation rate equation similar to Cu-17%Cr. This is consistent with the observation of Cu_2O in the exterior scale. At and below 873 K, thin discontinuous oxide scales form on the free surfaces of the alloy specimens as Al and Cu atoms migrate and react with oxygen at the surface to form Cu_2O scales with increasing Al content from the external surface to the interior (Fig. 16(b)). Theoretical calculations by Wright and Nelson [17] predict that the presence of Al atoms leads to the formation of neutral $(\text{Al}_{\text{Cu}}+2\text{V}_{\text{Cu}})$ complexes with a large binding energy of 320 kJ mol^{-1} in Cu_2O thereby inhibiting the diffusion of copper vacancies and copper atoms in the oxide. Since the scale was not discernable at and below 873 K, it is hypothesized that Al atoms bind the copper vacancies in the Cu_2O scale forming neutral $(\text{Al}_{\text{Cu}}+2\text{V}_{\text{Cu}})$ complexes as well as in the matrix thereby slowing down the diffusion of Cu in the oxide scale and in the matrix. As a result, scale growth is considerably diminished and void nucleation is suppressed in the matrix. Based on this rationale, it is expected that a critical amount of Al would be required to ensure that the alloy develops a significant oxidation resistance which is consistent with experimental observations that the critical amount of Al $> 2.5\%$ [13]. In addition, it is expected that void nucleation would be suppressed when the Al content exceeds a certain critical value.

Between 873 and 1073 K, the Al content of the scale increases especially in the layer near to the matrix-scale interface with increasing Al diffusion rate (Fig. 16(c)). Above 1073 K, an almost pure Al_2O_3 protective layer forms at the matrix-scale interface (Fig. 16(d)). Increased

diffusion of Cr with increasing temperature leads to a progressive enrichment of Cr in the middle and outer layers of the scale thereby leaving behind an almost pure Al_2O_3 subsurface layer.

Summary and Conclusions

The nature of the scale microstructures formed on Cu-17%Cr and Cu-17%Cr-5%Al alloys after oxidation between 773 and 1173 K are discussed. The scales formed on Cu-17%Cr consisted of external CuO and internal subsurface Cu_2O layers, where the scale thickness varied between 10 and 450 μm in the temperature range 773 -973 K. A large number of voids were observed around the original α -Cr particles and at the interfaces. A continuous protective Cr_2O_3 subsurface layer was not observed. In contrast, the Cu-17%Cr-5%Al formed very thin scales, which were not often discernable or continuous at the lower temperatures. Owing to the thinness of the scales, it was not possible to determine their compositions either by x-ray diffraction or by electron microprobe analysis. No voids were observed in the oxidized specimens. The EDS results revealed that the Al content of the scale increased with increasing temperature and increasing distance from the external surface towards the matrix with a corresponding decrease in their Cu content, where alumina scales were observed above 973 K. The results from energy dispersive spectra determined from the scales were used to construct an approximate scale composition map. Phenomenological mechanisms are proposed to understand the differences in the oxidation behavior of these alloys. It is proposed that the presence of Al in the alloy acts in two ways to improve the oxidation resistance of the alloy. First, Al binds the copper vacancies both in the matrix and in the Cu_2O scale thereby inhibiting the diffusion of Cu atoms and the formation of voids in the alloy. This mechanism appears to be important at the lower

temperatures where Al diffusion rate is low. Second, Al helps to form protective alumina subsurface scales at the higher temperatures.

Acknowledgements

The author thanks Ms. Joy Buehler for metallographic preparation of the specimens, Mr. Terry McCue for conducting the SEM observations and EDS analyses and the late Mr. Ralph Garlick for conducting x-ray diffraction analyses of the oxidized specimens. The author also thanks the reviewer for his valuable suggestions and comments.

References

1. G. Valensi, *Pittsburgh International Conference on Surface Reactions*, Electrochemical Society, Pittsburgh, PA (1948).
2. R. F. Tylecote, *J. Inst. Metals* **78**, 327-350 (1950-51).
3. D. W. Bridges, J. P. Baur, G. S. Baur and W. M. Fassell, *J. Electrochem. Soc.* **103**, 475-478 (1956).
4. S. Mrowec and A. Stoklosa, *Oxid. Metals* **3**, 291-311 (1971).
5. F. Gesmundo, C. De Asmundis and S. Merlo, *Werkstoffe Und Korrosion - Materials and Corrosion* vol 30, 114 (1979).
6. K. T. Chiang, K. J. Kallenborn, J. L. Yuen and N. E. Paton, *Mater. Sci. Eng. A* **156**, 85-90 (1992).
7. J. H. Park and K. Natesan, *Oxid. Metals* **39**, 411-435 (1993).
8. Y. Niu, F. Gesmundo, F. Viani and D. L. Douglass, *Oxid. Metals* **48**, 357-380 (1997).
9. K. T. Chiang, G. H. Meier and F. S. Pettit in: S. B. Newcombe and J. A. Little (Eds.) *Microscopy of Oxidation-3*, pp. 443-451 (The Institute of Metals, London, U.K., 1997).
10. Y. Zhu, K. Mimura, J. W. Lim, M. Isshiki and Q. Jiang, *Metall. Mater. Trans. A* **37A**, 1231-1237 (2006).
11. Y. Niu, S. Y. Wang and F. Gesmundo, *Oxid. Metals* **65**, 285-306 (2006).
12. S. Y. Wang, F. Gesmundo, W. T. Wu and Y. Niu, *Scripta Mater.* **54**, 1563-1568 (2006).
13. G. Plascencia, T. Utigard and T. Marín, *JOM* **57**, 80-84 (2005).
14. G. Ghosh in: G. Petzow and G. Effenberg, (Eds.), *Handbook of Ternary Alloy Phase Diagrams*, vol. 4 (VCH Publishers, New York, NY, 1991) pp. 311-319.
15. B. Grushko, E. Kowalska-Strzeciwiłk, B. Przepiorzynski and M. Surowiec, *J. Alloys and Compounds* **417**, 121-126 (2006).
16. K. T. Chiang, K. J. Kallenborn and J. L. Yuen, *Surf. Coat. Tech.* **52**, 135-139 (1992).
17. A. F. Wright and J. S. Nelso, *J. Appl. Phys.* **92**, 5849-5851 (2002).

Table 1: X-ray diffraction results from the surfaces of oxidized Cu-17%Cr and Cu-17%Cr-5%Al after 100 h.

Alloy	Temperature (K)				
	773	873	973	1073	1173
Cu-17%Cr	α -Cr (w) α -Cu (w) Cu ₂ O (m) CuO (s)	Cu ₂ O (w) CuO (s)	Cu ₂ O (w) CuO (s)		
Cu-17%Cr-5%Al	α -Cr (s) α -Cu (s)	α -Cr (s) α -Cu (s)	α -Cr (s) α -Cu (s)	α -Cr (s) α -Cu (s) CuO (w)	α -Cr (s) α -Cu (s)

Note on peak intensities: m = medium; s = strong; w = weak.

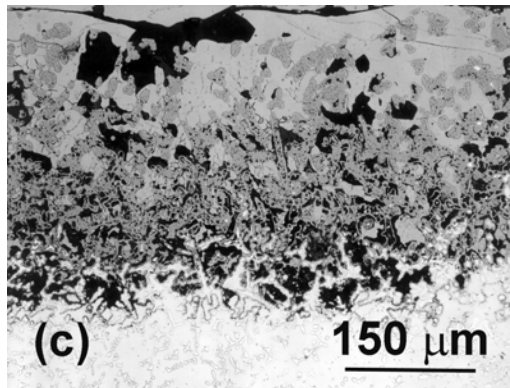
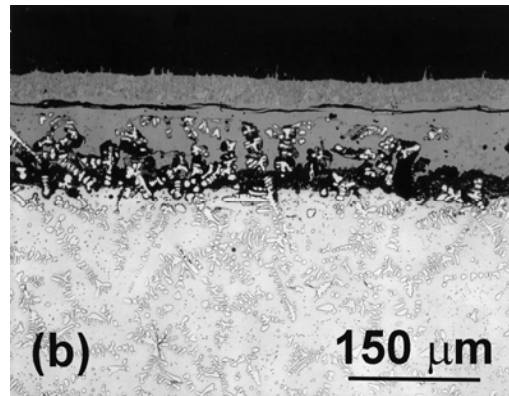
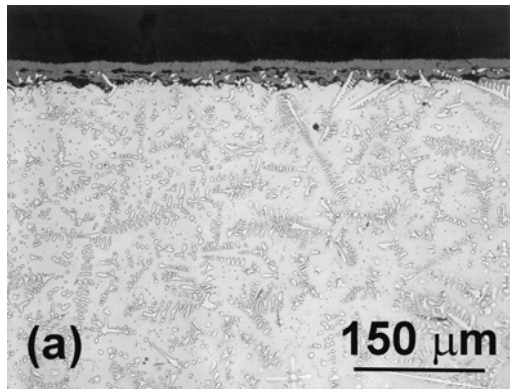


Fig. 1 Optical micrographs showing the scale microstructures for Cu-17%Cr after oxidation at (a) 773 K, (b) 873 K and (c) 973 K for 100 h.

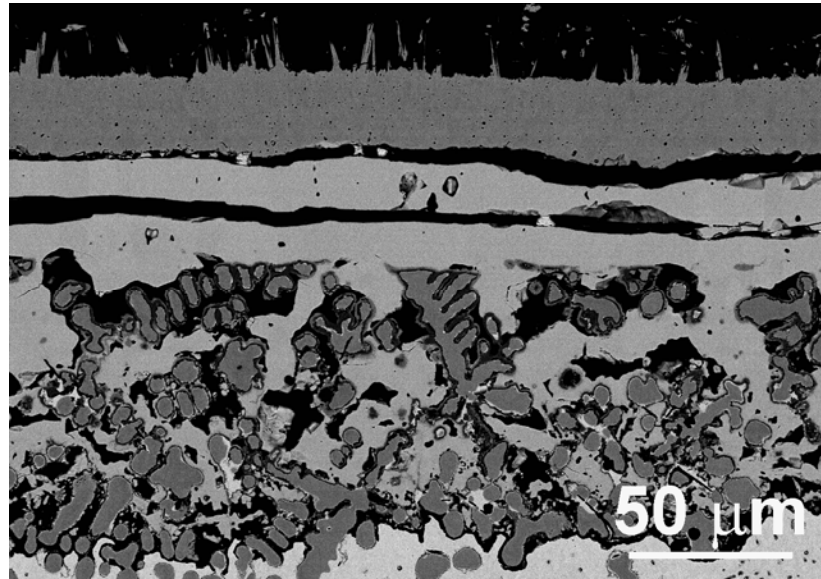


Fig. 2 Back scattered electron image of the scale microstructure formed on Cu-17%Cr after oxidation at 873 K for 100 h showing an absence α -Cr particles in the exterior layers.

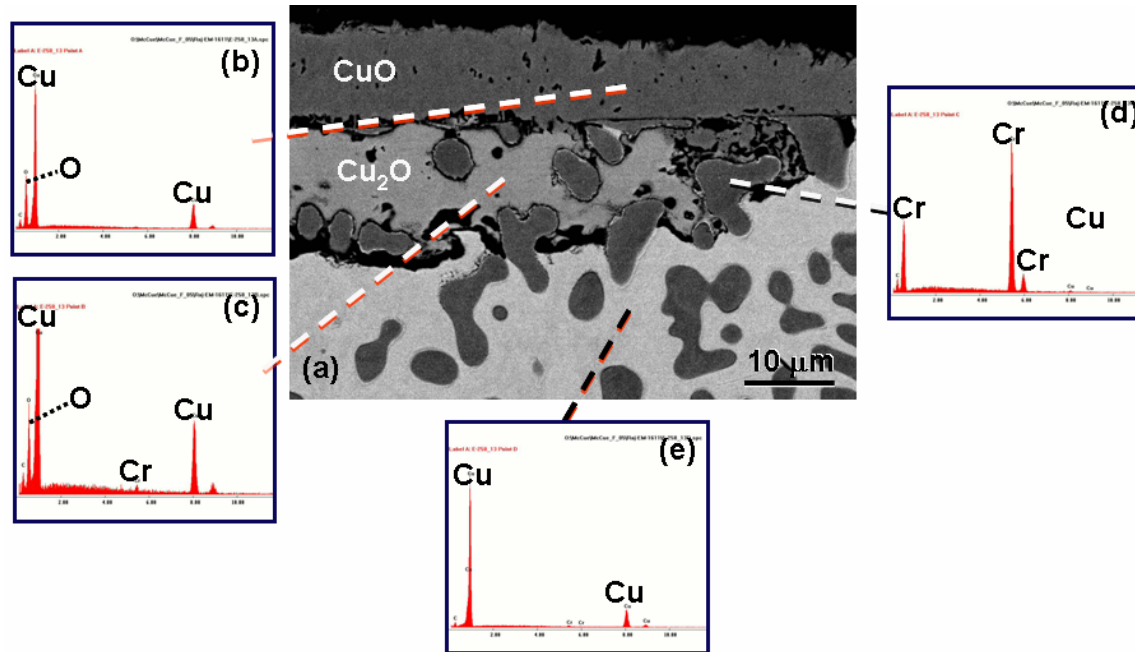


Fig. 3 Back scattered electron image and corresponding energy dispersive spectra of the scale formed on Cu-17%Cr oxidized at 773 K for 100 h.

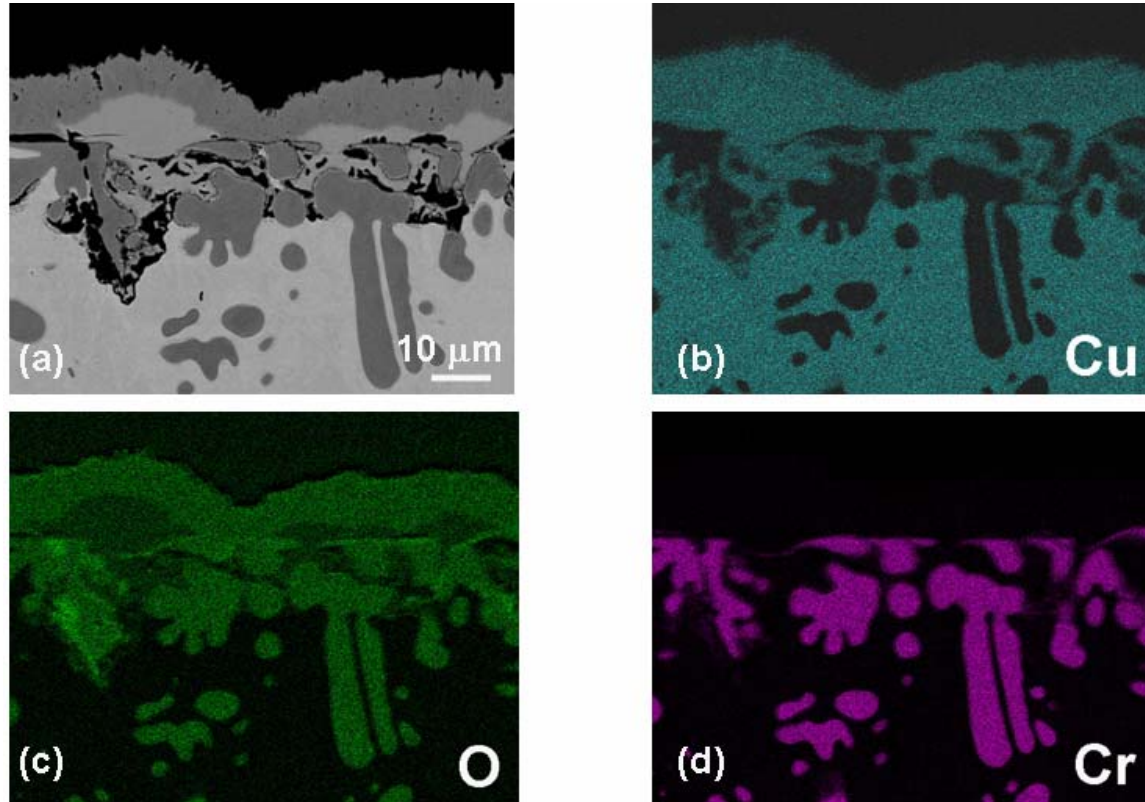


Fig. 4 (a) Back scattered electron image, and (b) Cu, (c) O and (d) Cr elemental x-ray maps of the scale formed on Cu-17%Cr oxidized at 773 K for 100 h showing the presence of oxidized α -Cr particles. The bright regions corresponding to the second phase in (c) are probably due to Cr L_{α} rather than O K_{α} reflections.

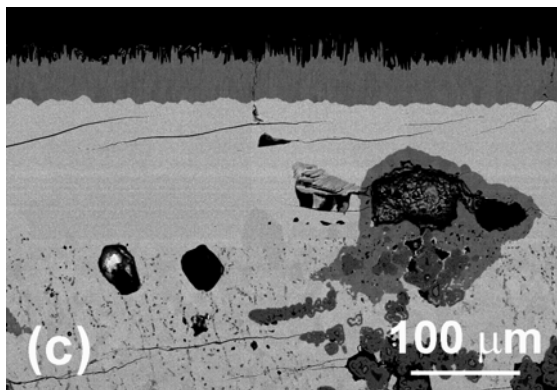
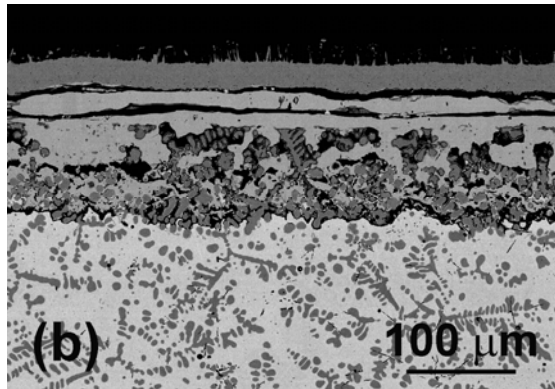
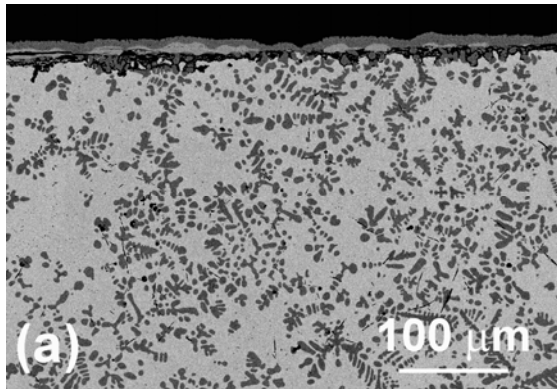


Fig. 5 Back scattered electron images of the scales formed on Cu-17%Cr specimens oxidized at (a) 773 K, (b) 873 K and (c) 973 K for 100 h.

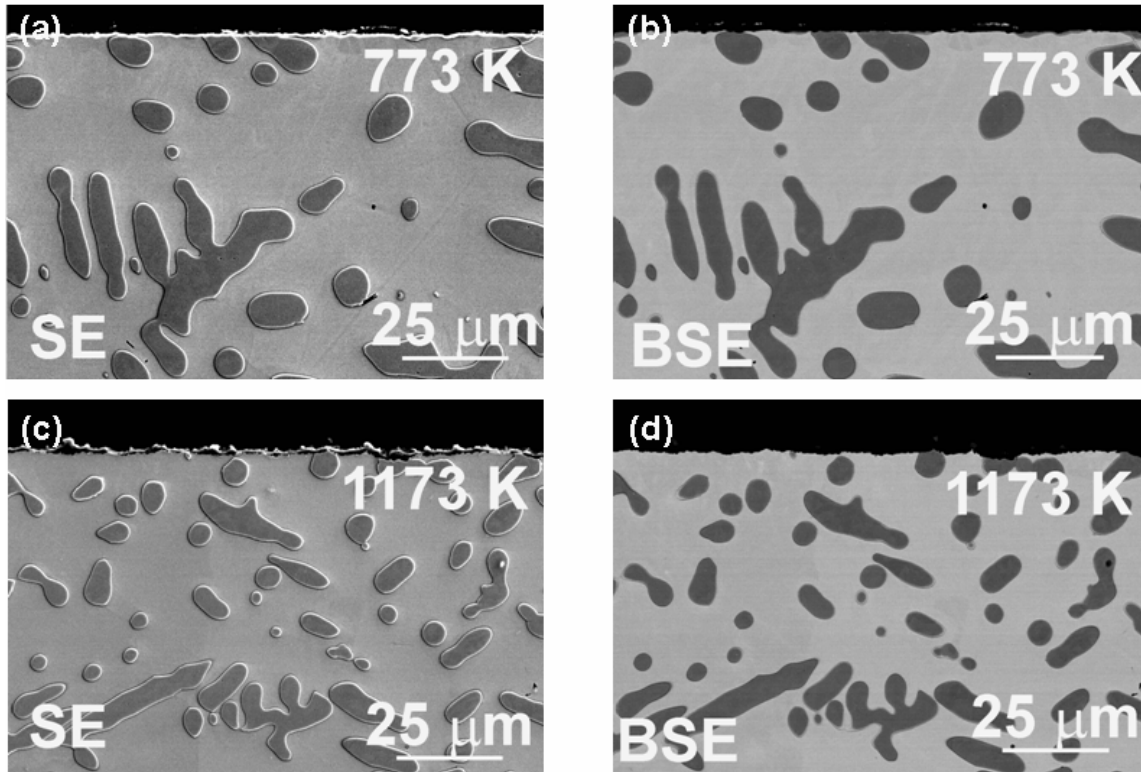


Fig. 6 Scanning and back scattered electron imaged microstructures of Cu-17%Cr-5%Al specimens oxidized at (a) & (b) 773 K and (c) & (d) 1173 K.

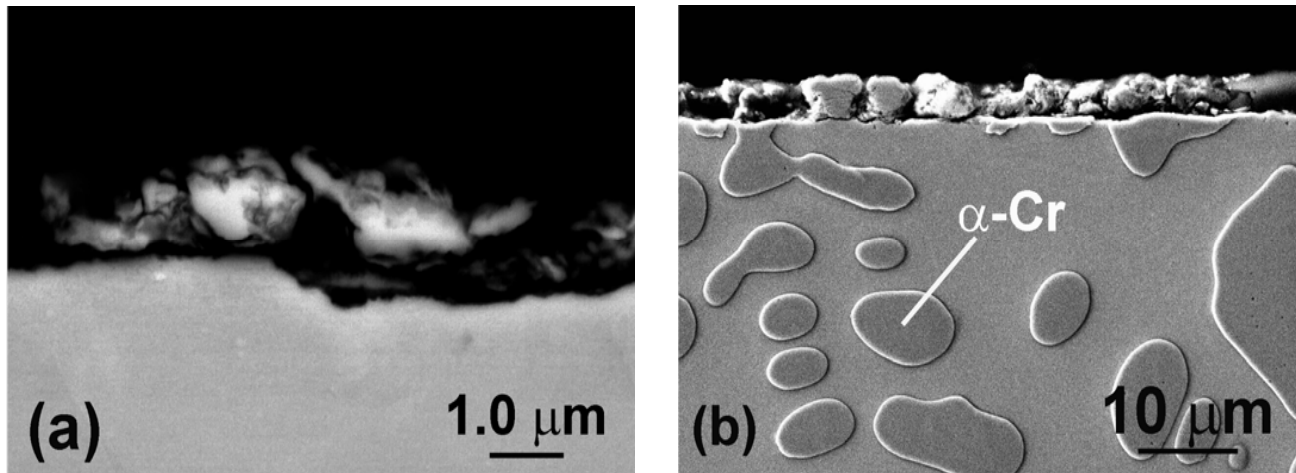


Fig. 7 Microstructures of Cu-17%Cr-5%Al specimens oxidized at (a) 773 K and (b) 873 K for 100 h showing the non-uniform and discontinuous morphology of the scales; (a) & (b) are back scattered and secondary electron images, respectively.

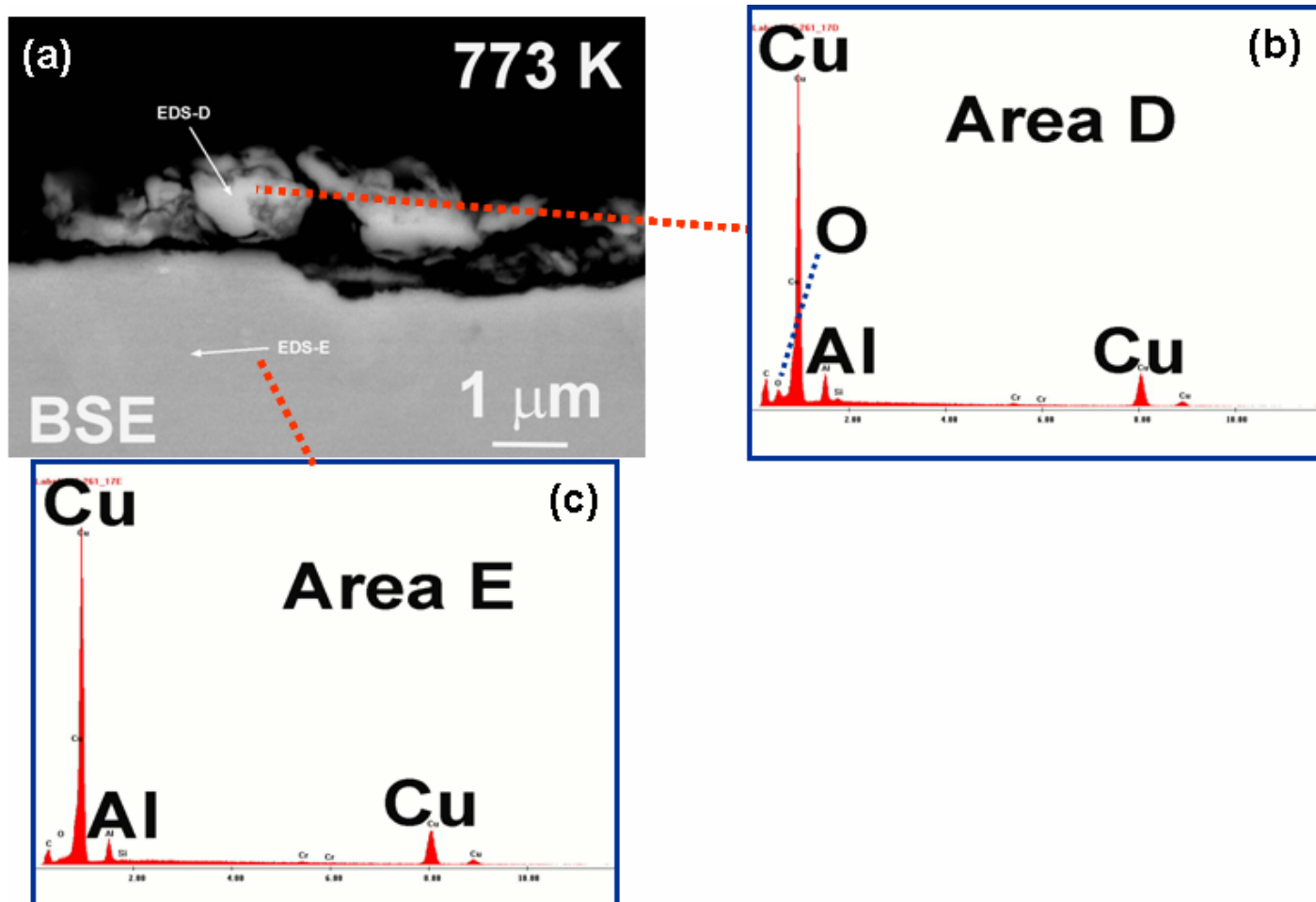


Fig. 8 Energy dispersive spectra from an area of the scale formed on Cu-17%Cr-5%Al oxidized at 773 K for 100 h.

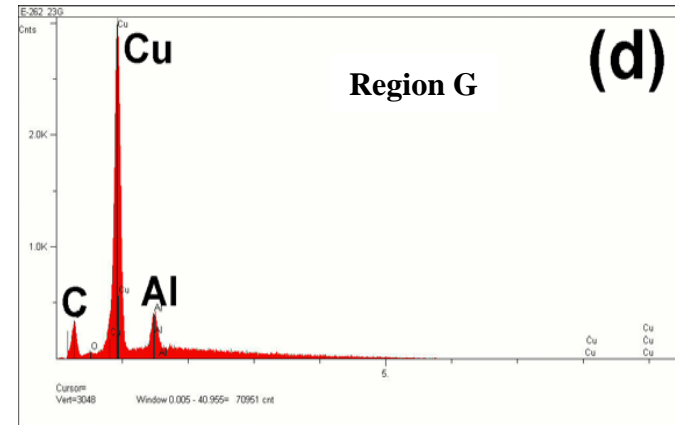
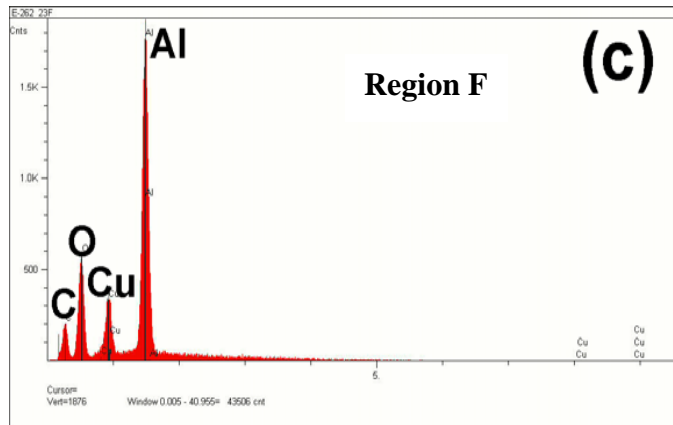
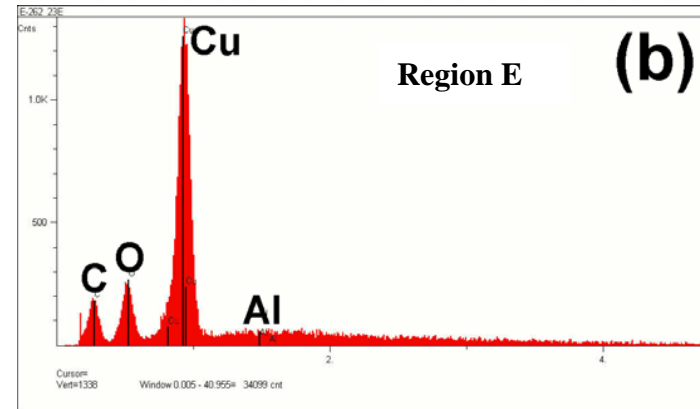
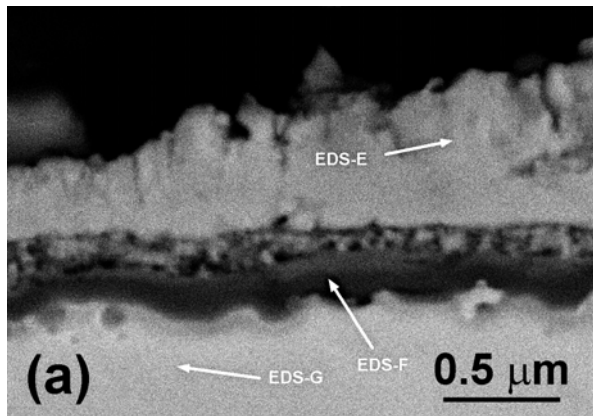


Fig. 9 (a) Scanning electron micrograph of the scale formed on a Cu-17%Cr-5%Al specimen oxidized at 873 K for 100 h; (b), (c), (d) energy dispersive spectra from regions E, F and G, respectively.

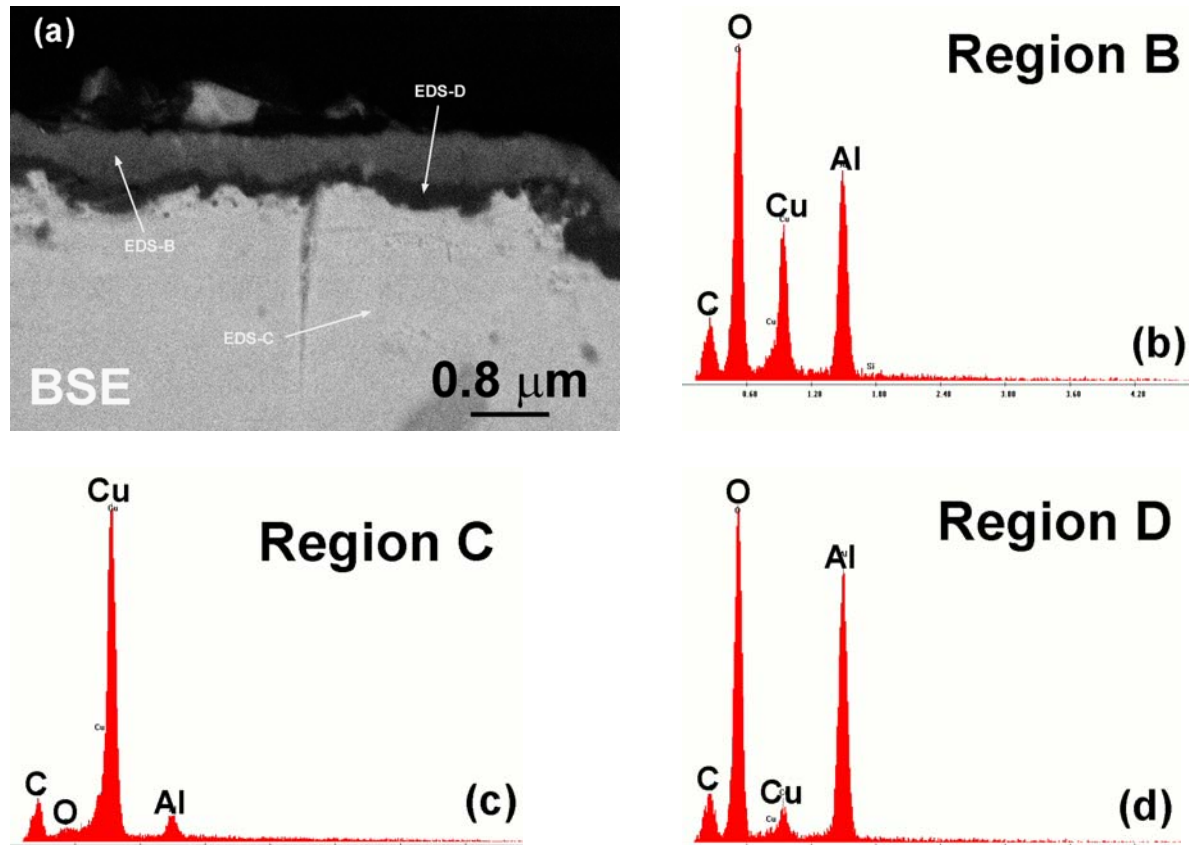


Fig. 10 (a) Back scattered electron image showing microstructure of the oxide scale formed on a Cu-17%Cr-5%Al specimen oxidized at 973 K for 100 h. (b), (c) and (d) energy dispersive spectra from regions B, C and D, respectively. The peaks on the far left are from the carbon coating on the specimen.

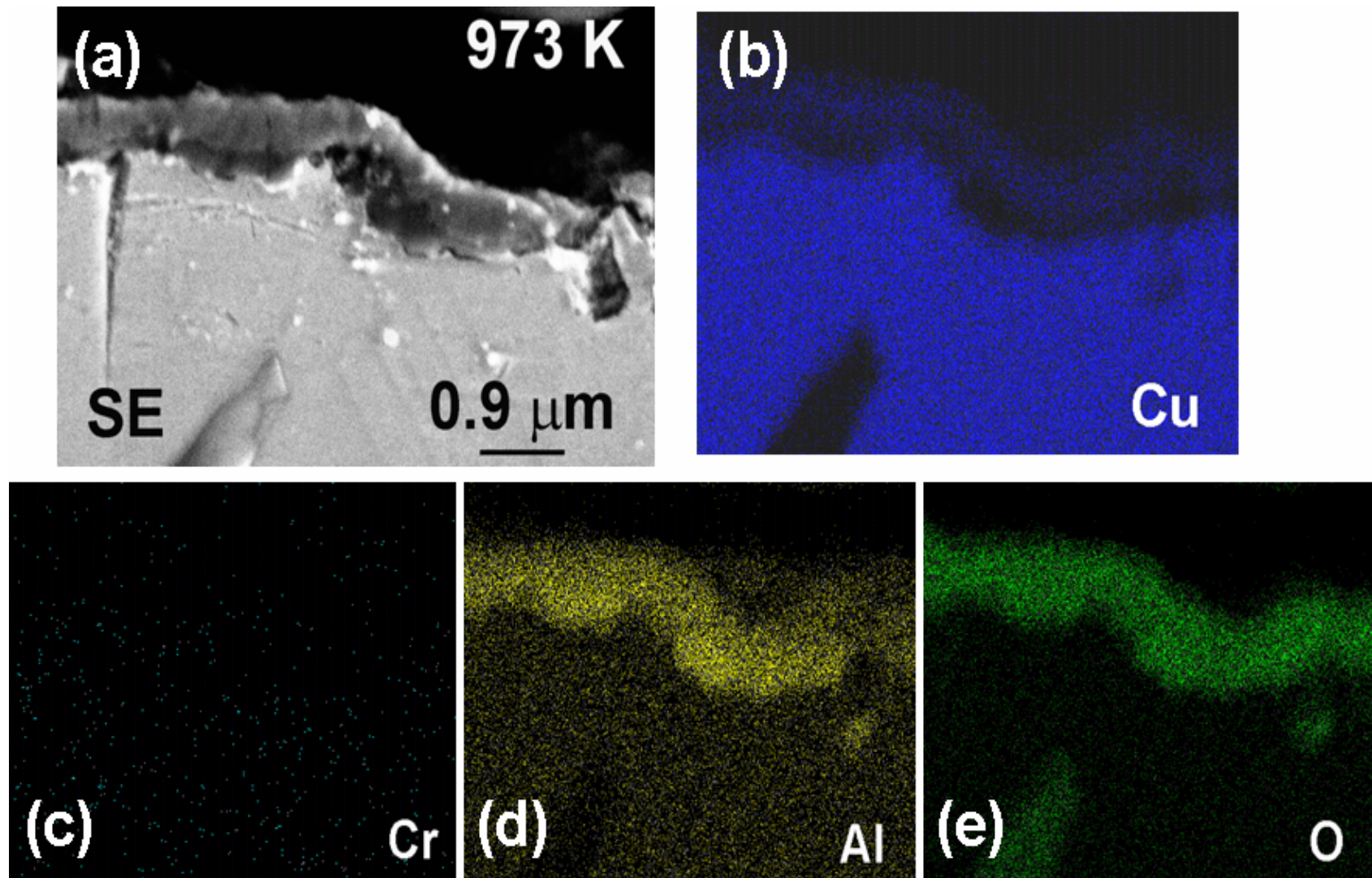


Fig. 11 Elemental x-ray maps of the scale formed on Cu-17%Cr-5%Al oxidized at 973 K for 100 h.

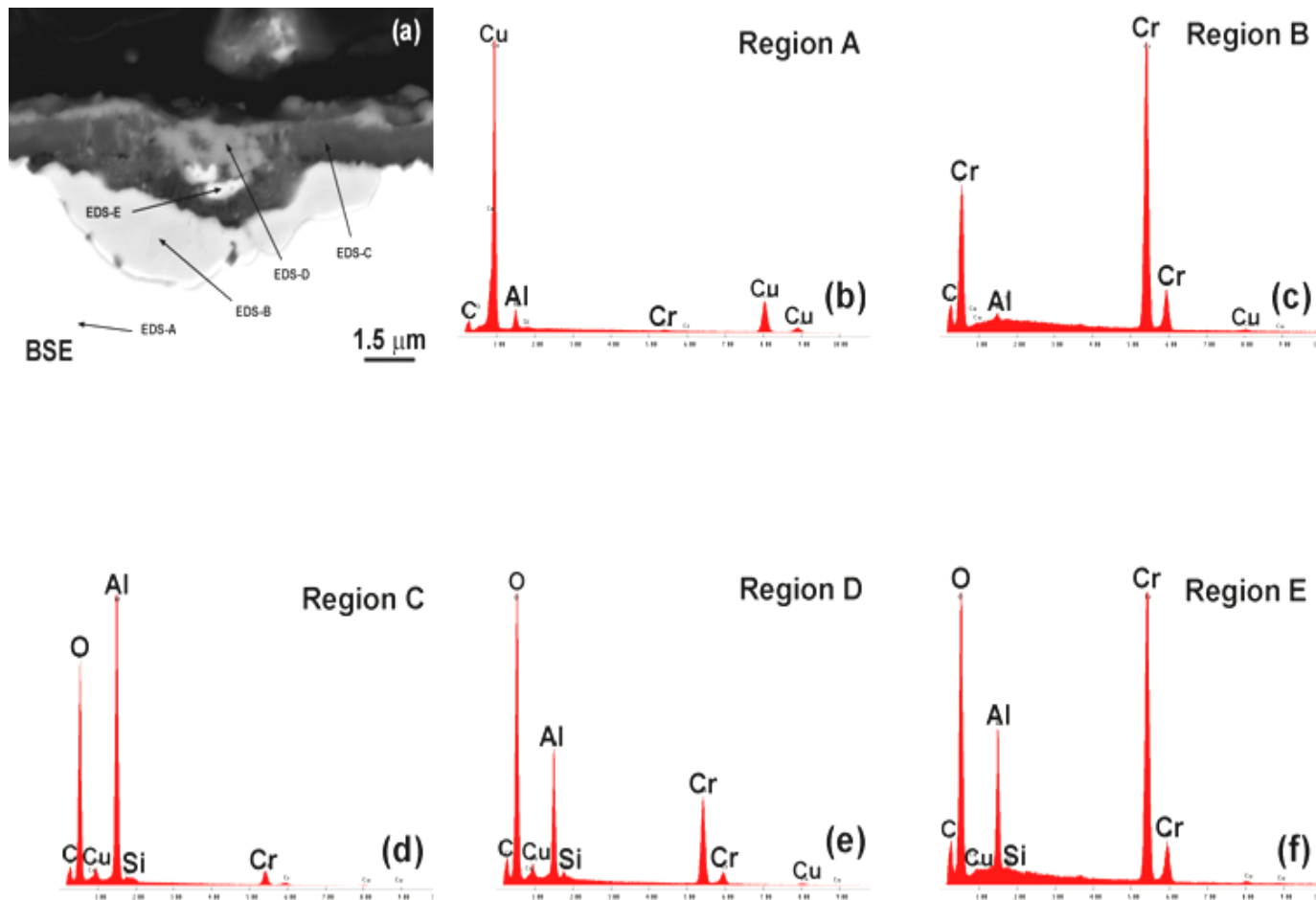


Fig. 12 (a) Back scattered electron image showing microstructure of the oxide scale formed on a Cu-17%Cr-5%Al specimen oxidized at 1073 K for 100 h. (b), (c), (d), (e) and (f) energy dispersive spectra from regions A, B, C, D and E, respectively. The peaks on the far left are from the carbon coating on the specimen, while the Si peak is most likely due to colloidal silica left over from the metallographic preparation process.

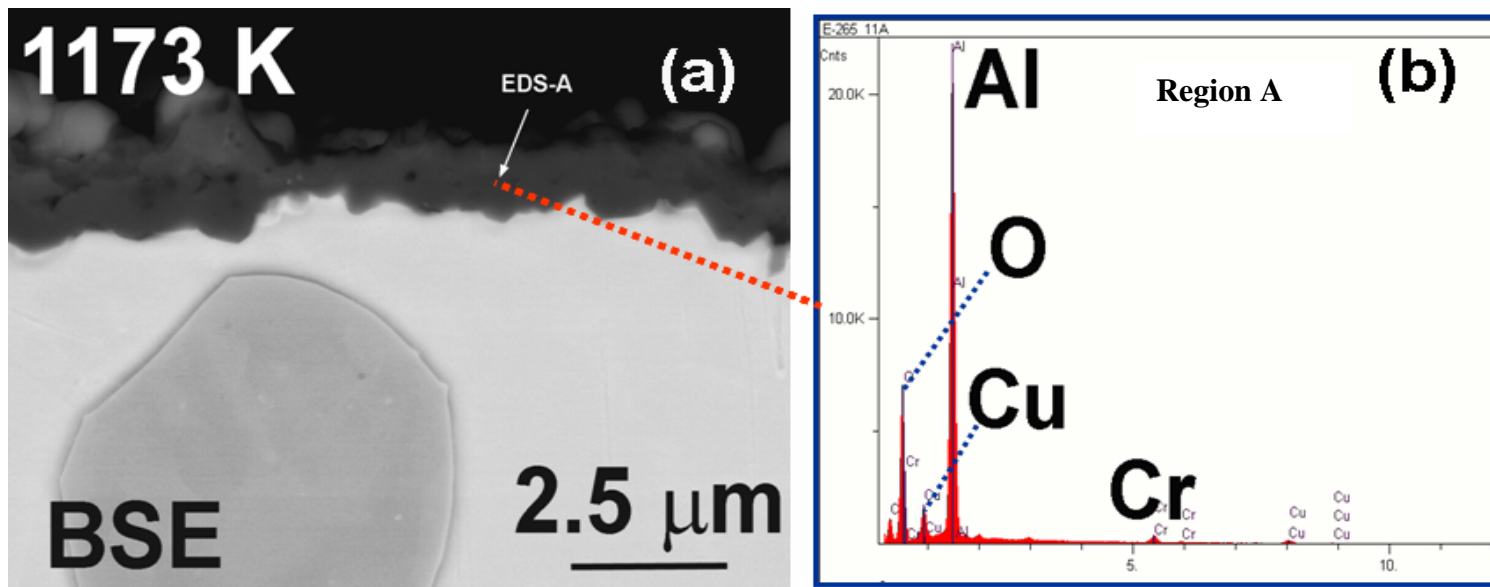


Fig. 13 Composition of the scale formed on Cu-17%Cr-5%Al oxidized at 1173 K for 100 h.

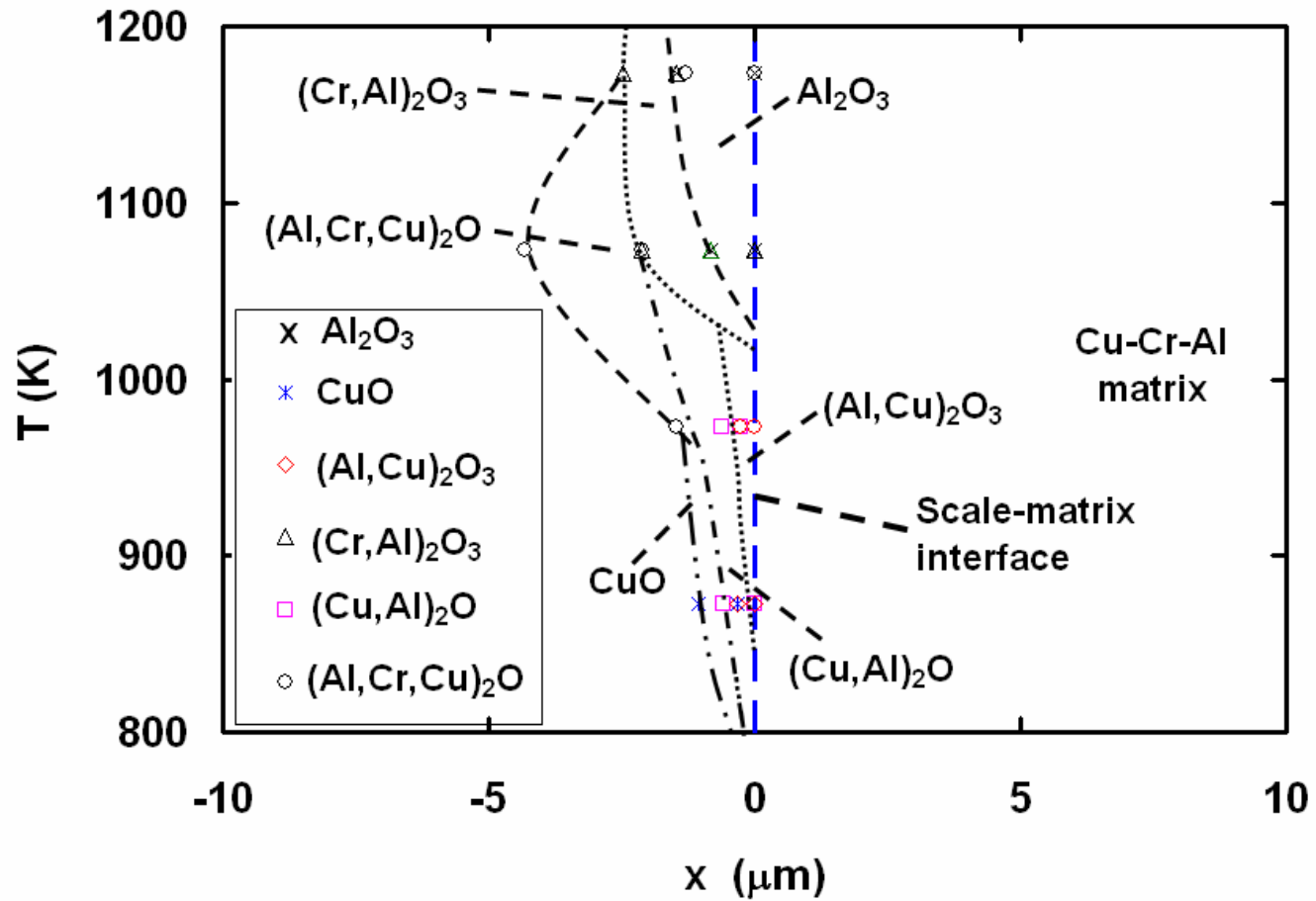


Fig. 14 Oxide scale composition map for Cu-17%Cr-5%Al, where x represents the local distance from the matrix-scale interface.

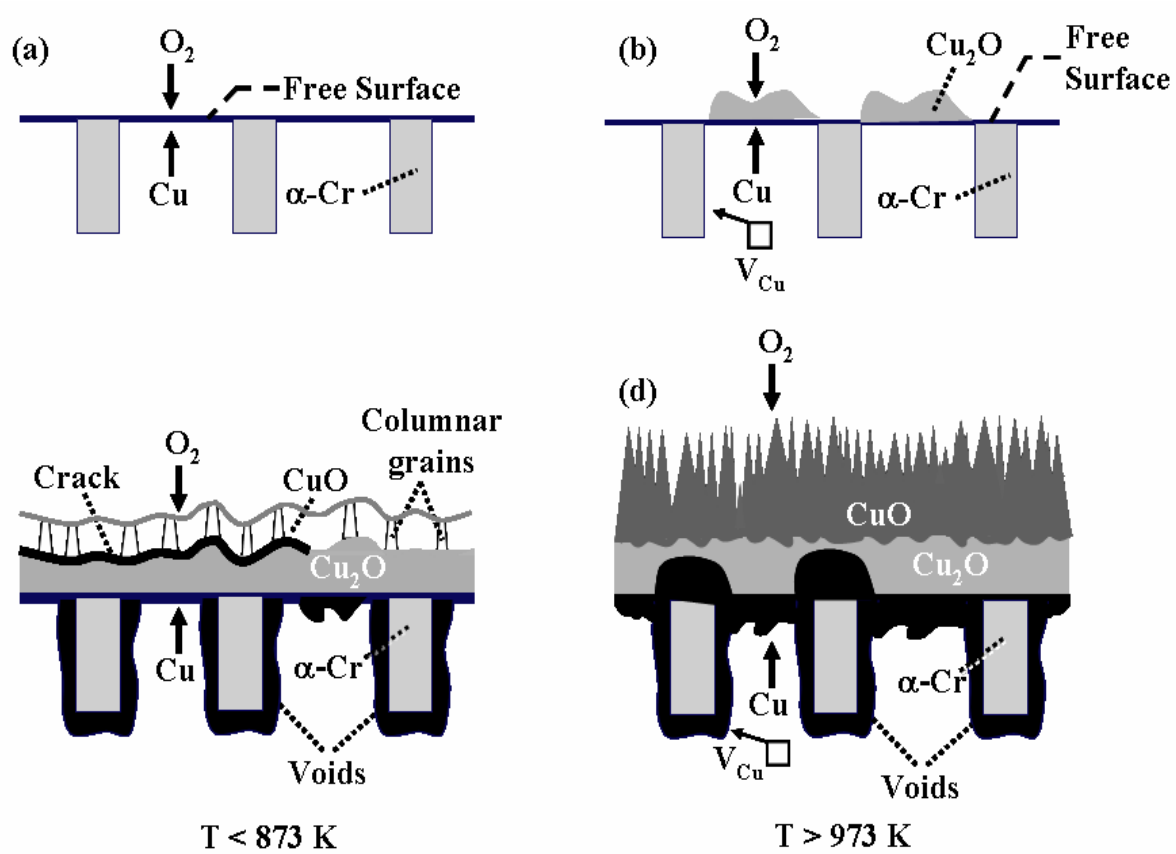


Fig. 15 Schematic illustrating the formation of an oxide scale on as-cast Cu-17%Cr. (a) Virgin surface undergoing oxidation; (b) Cu atom diffusion to the free surface leads to the formation of a Cu_2O scale at the surface and copper vacancies, V_{Cu} , in the matrix; (c) & (d) formation of columnar grain growth in the CuO exterior scale during later stages of oxidation with corresponding void formation at the interfaces due to vacancy accumulation.

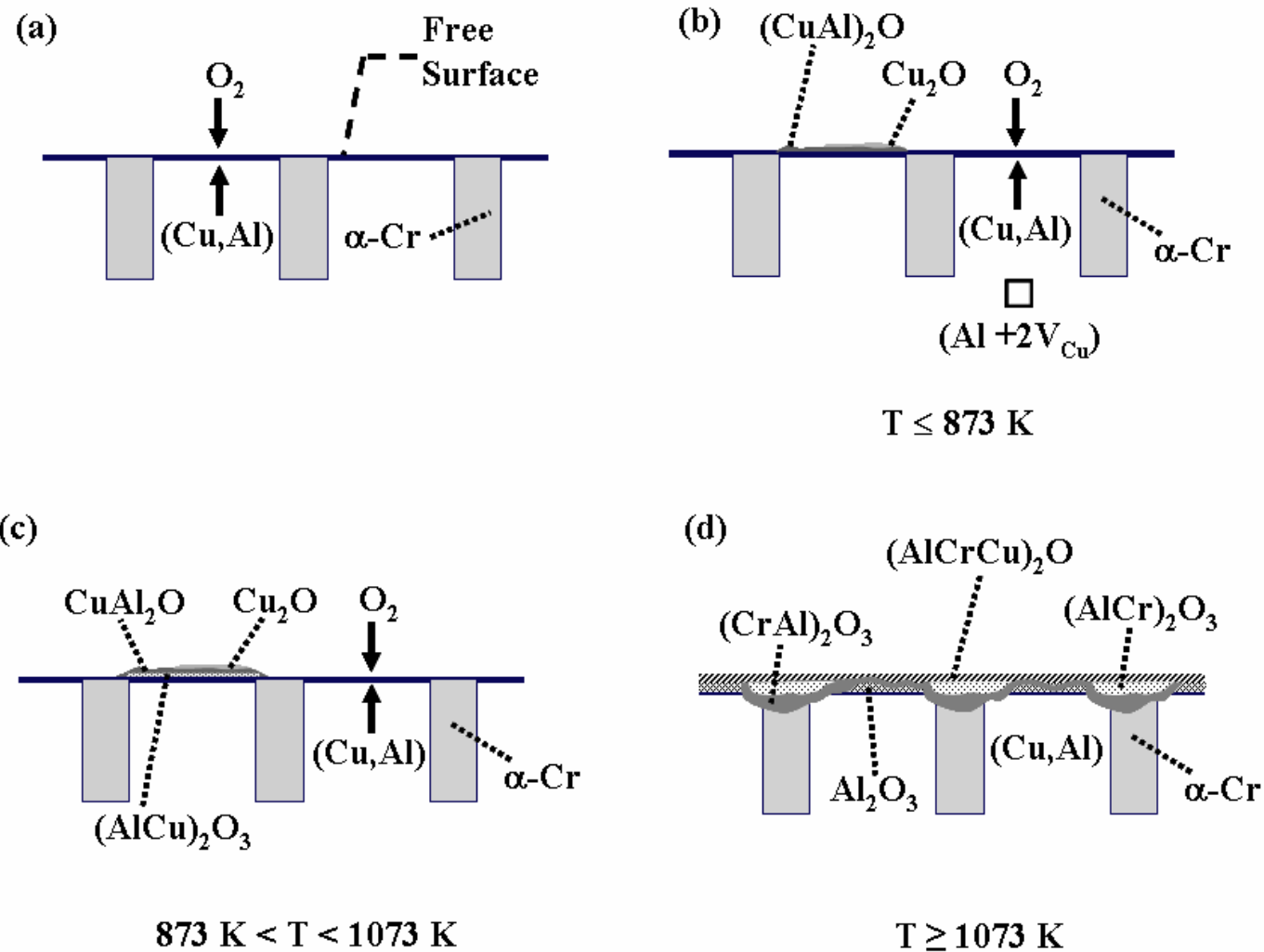


Fig. 16 Schematic illustrating the formation of an oxide scale on as-cast Cu-17%Cr-5%Al. (a) Virgin surface undergoing oxidation; (b) Cu atom diffusion to the free surface leads to the formation of an Al-deficient and Al-rich Cu_2O exterior and subsurface scale, respectively. Each Al atom binds two copper vacancies in the matrix thereby inhibiting the migration of Cu atoms and the formation of voids; (c) mixed oxide scales form between 873 and 1073 K during later stages of oxidation with the Al content of the scale increasing from the free surface to the scale-matrix interface; (d) Al and Cr-rich exterior scales and a protective alumina subsurface layer form during later stages of oxidation above 1073 K.